Materials Science Forum Vols. 192-194 (1995) pp. 421-432
© 1995 Trans Tech Publications, Switzerland

Pitting Corrosion of Laser Surface Modified Aluminium Alloys

M.G.S. Ferreira[1], R. Li[1], J.S. Fernandes[1], A. Almeida[1], R.Vilar[1], K.G. Watkins[2] and W.M. Steen[2]

[1] Instituto Superior Técnico, P-1096 Lisboa Codex, Portugal

[2] University of Liverpool, Liverpool L69 3BX, U.K.

Keywords: Aluminium Alloy, Laser Treatment, Pitting Corrosion

Introduction

Laser surface modification is a rapidly melting and a rapidly resolidifying process which can modify both the microstructure and the distribution and composition of alloying elements in the melted layer, affecting surface related properties such as wear and corrosion resistance. This has particular potential in the treatment of aluminium alloys [1-5] since most of the added alloying elements which are essential for the enhancement of strength compared to unalloyed aluminium invariably lower the resistance of the metal to corrosion.

The laser surface treatments take usully two different forms: laser alloying where foreign elements are added during the laser processing and laser melting where there is no addition of foreign elements during the processing. In this latter case only the microstructure and/or the distribution of the elements in the surface layer are changed. The present paper deals with laser surface melting (LSM) of 2024 aluminium alloy and laser surface alloying (LSA) of 7175 alloy with chromium by a CO_2 laser.

Experimental

Laser Processing

2024-T351 aluminium alloy plate with nominal composition as shown in Table 1 and dimensions 15 x 10 x 1.3 cm was laser surface melted using a continous wave CO_2 laser operating at 2kW by traversing the sample beneath the beam by means of a computer controlled X-Y table. The laser beam spot diameter was 1.5 mm and the traverse speed was 20 mm/s. Before laser treatment an amorphous carbon film was deposited by sooting in order to reduce reflectivity and enhance absorption of the energy from the laser. To

minimise oxidation during LSM, argon gas was blown over the molten pool.

Table 1 - Nominal composition of 2024 aluminium alloy

% Cu	% Mg	%Mn	%Al
4.4	1.5	0.6	bal

7175-T7351 aluminium alloy plate with nominal composition as shown in Table 2 was laser surface alloyed with chromium using the same CO_2 laser. The laser beam spot diameter was 1.5-2.0 mm and the traverse speed of the operating table was 10 mm/s. The chromium alloying element was supplied as powder and mixed with aluminium powder giving the composition Al-25 (wt%) Cr. The powder was blown to the melting pool with delivery gas and argon was blown over the melting pool to avoid oxidation of the samples during the processing.

To eliminate the defects in the alloyed layers they were laser remelted in a direction perpendicular to the direction used previously for alloying.

Table 2 - Nominal composition of 7175 aluminium alloy

% Cu	% Mg	% Si	% Fe	% Cr	% Zn	% Mn	% Al
1.2-2.0	2.1-2.9	0.15	0.20	0.18-0.28	5.1-6.1	0.1	bal.

Tests

The characterization of the microstructure was made by light microscopy and scanning electron microscopy after metallographic preparation and etching with Keller's reagent. The distribution and morphology of the intermetallic compounds were studied by SEM, using backscattered electrons images of unetched cross sections of melted tracks. The phase identification was carried out by x-ray diffraction and etching with selective reagents. Chemical analysis of the samples was performed using EDX and electron microprobe (EPMA). Microhardness measurements were made in some cases at the surface and cross section of the samples with a vickers indenter, under a

100 g load.

The pitting corrosion resistance of the specimens was evaluated by anodic polarization tests in 3 wt% NaCl dearated solution, using a conventioned three electrode cell, comprising the sample, a platinum foil counter electrode and a satured calomed reference electrode. The samples were previously mounted in epoxy resin, ground with emery paper to 1000 grit and polished with 3 μm diamond paste. The boundary between the sample and the epoxy resin was sealed with bee's wax to avoid crevice corrosion.

Before polarization the samples were immersed in the solution for 2 hours to stabilise the open circuit potential and then the potential was swept at a rate of 1,5 mV/min.

In some cases immersion tests were carried out by observing the variation of the free corrosion potential of the sample with time in naturally aerated 3% NaCl solution, and observing with SEM the specimens after the tests.

Results and Discussion

LSM 2024 Alloy

The operating conditions chosen produced a relatively thin surface melted layer whose microstructural characterization revealed denditric subgrains within the grain resulting in a very fine microstructure at the subgrain level, Fig.1. Two main phases were identified by x-ray diffraction: a dendritic phase based on the primary solid solution (α-Al) and a precipitated second phase which formed a continous network around the dendrite boundaries (θ-Al_2Cu). The second phase normally identified in non-laser surface melted 2024 aluminium alloy is S-phase (Al_2CuMg) [6]. However it is known that this phase will only form when the Mg:Cu ratio is above a critical level and hence, for example, it is the θ–Al_2 Cu phase which is present in 2014 alloy which has a lower ratio of Mg: Cu. Determination of the chemical composition of the 2024 alloy after LSM by EDX (Table 3) revealed that the Mg content had been lowered compared to the as received alloy (Table 1), probably as a result of selective vaporisation of Mg during laser melting. This lower Mg content is thus consistent with the presence of θ-Al_2Cu in the laser melted alloy.

Fig. 1 - Microstructure of laser surface melted layer Δ: $CuAl_2$

Table 3 - Composition of the laser melted layer by EDX

% Cu	% Mg	%Mn	% Cr	% Al
4.3	0.7	0.8	0.1	bal.

Anodic polarization plots obtained after immersion in 3% NaCl solution for untreated and treated specimens are shown in Fig. 2 [7]. There is an anodic current transient at -652 mv for the as received sample and the pitting potential is -604 mv. No anodic current density transient was observed on the laser surface melted sample and the pitting potential is -635 mv. For the as received material a large number of pits are formed along the rolling direction and a smaller number of pits are formed in other places. At higher magnification, intergranular corrosion, can also be seen, Fig. 3.

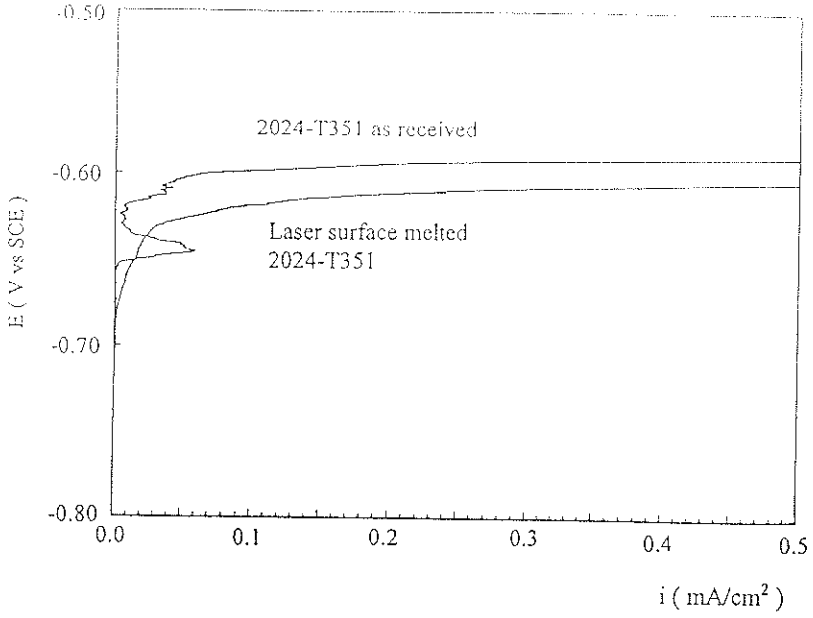

Fig. 2 - Anodic polarization curves of 2024-T351 as received and laser surface melted in dearated 3% NaCl.

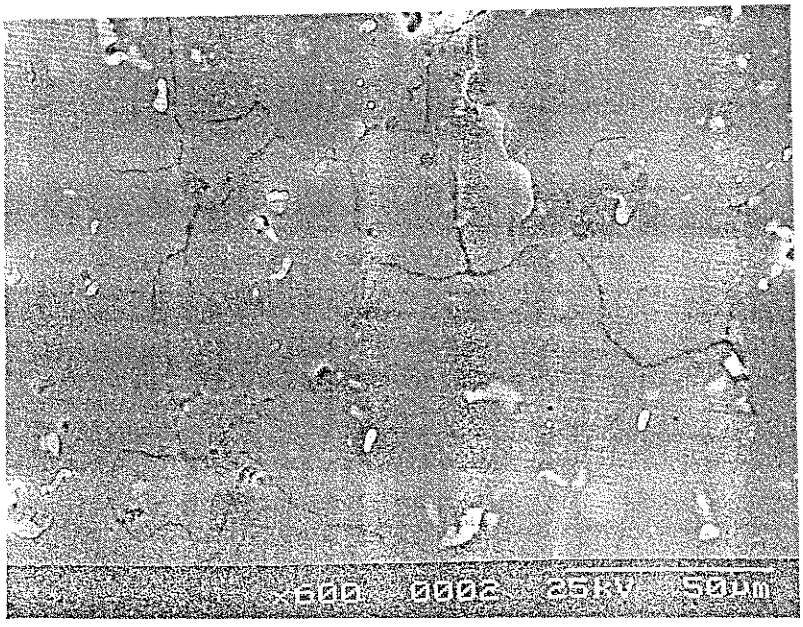

Fig. 3 - Pitting and intergranular corrosion on 2024-T351 alloy as received after anodic polarization in dearated 3% NaCl

In the LSM sample only pitting corrosion occurred in the form of clusters of smaller pits distributed in a grid pattern on the surface. It has been shown [6] for aged Al-Cu-Mg alloys in NaCl solution that the current transient on anodic polarization is attributable to the pitting corrosion of grain boundary Al_2CuMg precipitates since the pitting potential of such precipitates is lower than that of the α-Al primary solid solution grains. In the present work in the as received condition the commercial 2024-T351 aluminium alloy which was used contained some coarse undissolved precipitates, mainly Al_2CuMg, distributed along the rolling direction and a large amount of much smaller Al_2CuMg precipitates at the grain boundaries resulting from the aging process. Since the pitting potential of Al_2CuMg precipitates is lower than that of the α-Al matrix it would be expected that pitting corrosion should be initiated at both the larger and the finer grain boundary Al_2CuMg precipitates in the as received alloy. This process is responsible for the current transient on anodic polarization. Propagation of the pits at the grain boundary leads to the observation of intergranular corrosion. Since the both larger undissolved precipitates along the rolling direction and the finer grain boundary precipitates resulting from the aging process are present both pitting corrosion and intergranular corrosion are observed.

The modified microstructure that forms as a result of LSM of the aluminium alloy contains Al_2Cu instead of Al_2CuMg, since the Mg content of the alloy lowered substantially as a result of selective vaporization. Al_2Cu is cathodic relatively to the α-Al dendrites [6] leading to the onset of pitting in this latter phase. Thus a single breakdown potential is detected.

Since pitting does not take place at the site of the precipitates there is no current transient in the anodic polarization curve and a single breakdown potential is observed.

The variation of potential with time during immersion tests in naturally aerated 3% NaCl solution for the as received and laser melted samples are depicted in Fig. 4 and reveal a different behaviour for these materials when time elapses. Initially the evolution of potential with time is similar showing an enobling of the potential for the first 350 s. Then the potential is kept nearly contant up to 1000 sec, although in the case of the as received material fluctuations of potential are more apparent. After this period of time the potential falls sharply in the as received specimen whereas in the laser surface melted alloy no sharp decline could be seen. This behaviour was explained [7] on the basis of two competitive processes: one is the growth of the passive film on the alloy and/or the preferential dissolution of Al and Mg with eventual Cu enrichment and thus potential enobling and the other one is the decrease of

pH in the pits, due to the hydrolisis of the corrosion products, that stabilises the metastable pits forming and thus leading to a decrease of potential. The predominance of any of these processes or the balance between them will explain the observed evolution of potential with time [7]. Apart from the explanation for the phenomena SEM observation revealed after 8 hours immersion for the as received material a high density of small pits (20-50 μm diameter) and simultaneously intergranular corrosion whereas for the laser surface melted sample a lower density of larger pits (50-150 μm) were observed without any evidence if intergranular corrosion [7].

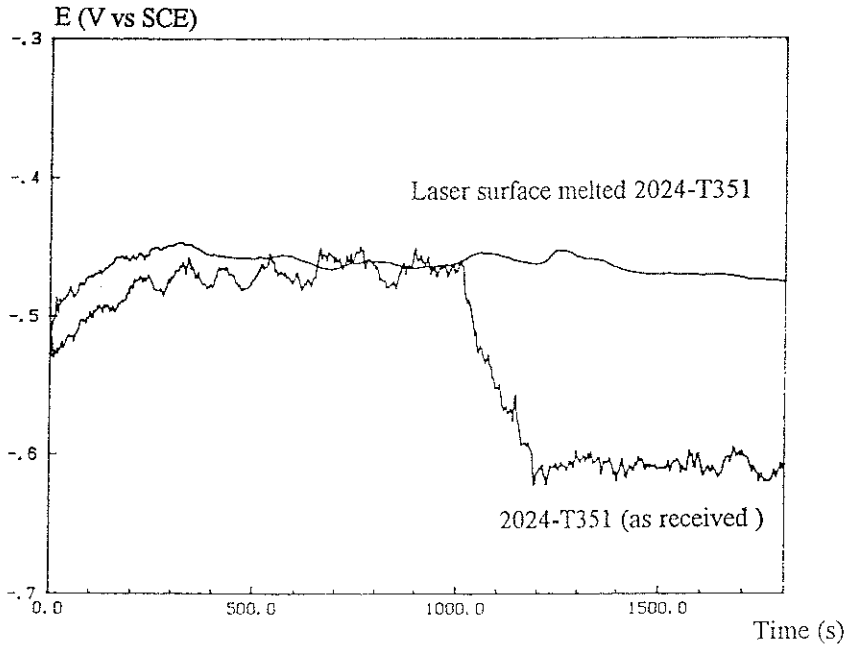

Fig. 4 - Potential Vs time curves for 2024-T351 as received and laser surface melted in naturally aerated 3% NaCl [7].

LSA 7175

In the alloyed and remelted layer the microstructure is very fine showing a cellular equiaxed morphology, with intermetallics organized radially around primary cubic particles, Fig. 5, whereas beneath in the layer only alloyed a network of long faceted intermetallic compound needles dispersed in a matrix of aluminium can be observed, Fig. 6. The intermetallic compounds identified

by x-ray diffraction were θ - Al_7Cr and η - $Al_{11}Cr_2$ [8]. In the method layer traces of ε - Al_4Cr were also found.

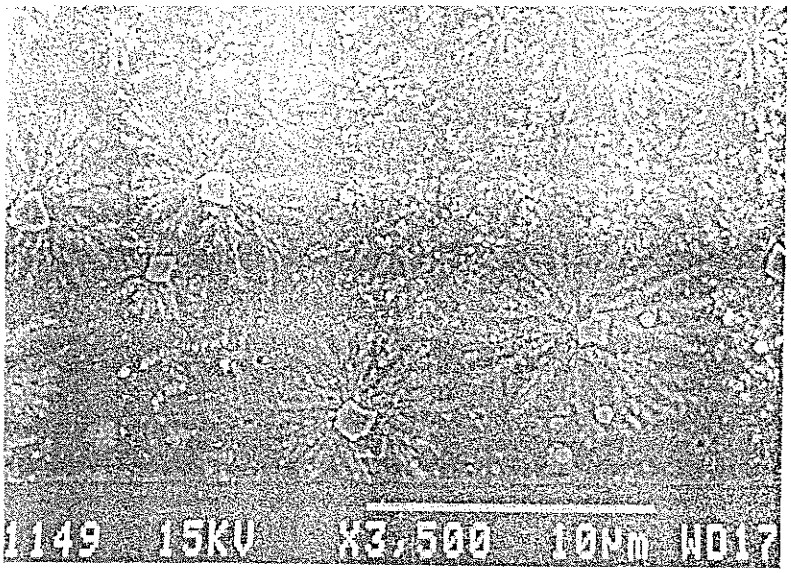

Fig. 5 - Cellular structure at the top of the aluminium-chromium alloyed and remelted layer with radial intermetallics around primary cubic particles [8].

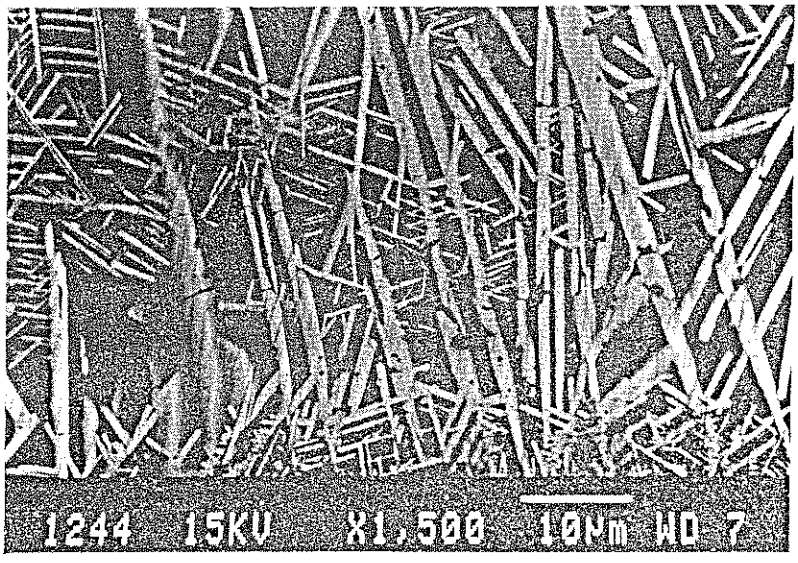

Fig. 6 - Needle shaped intermetallics at the top of the aluminium-chromium alloyed layer [8]

A typical hardness profile along the depth of the cross section of the alloyed tracks is depicted in Fig. 7. Laser alloying increases considerably the hardness of the base material, from 155 to about 310 HV. The increase of hardness depends on the chrominum content in the alloy, increasing with this one [8].

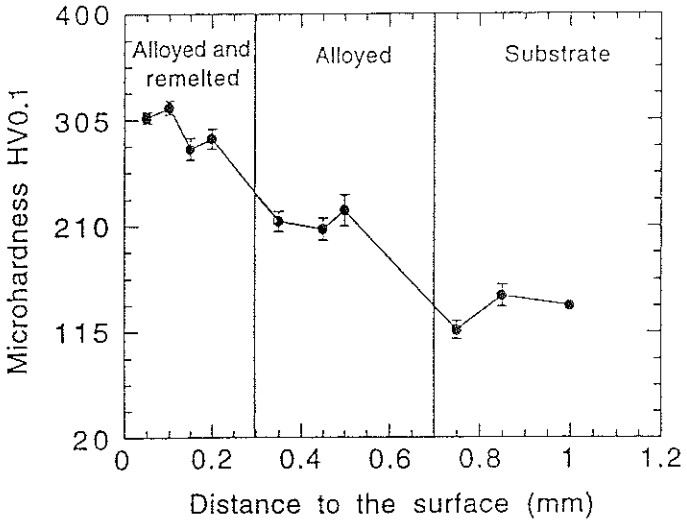

Fig. 7 - Microhardness profile of laser alloyed 7175 alloy with chromium

Fig. 8 shows anodic polarization curves for 7175 alloy before and after laser alloying with chromium. The pitting potential of untreated 7175 alloy is -730 mV, while in the chromium - alloyed layers increases to -620, -380 and -270 mV for chromium concentration of 5, 10 and 12 wt% respectively. The results make apparent that laser surface alloying improves the resistance to pitting corrosion initiation and that this effect increases with the chromium content.

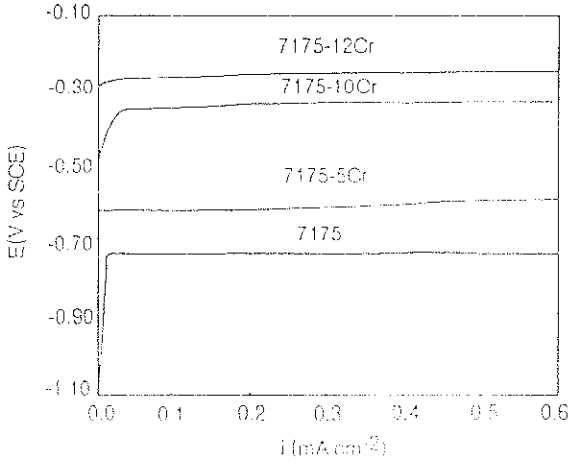

Fig. 8 - Anodic polarization curves for laser chromium-alloyed 7175 alloy [8]

Fig. 9 shows that the pits nucleate at the matrix, which has lower chromium content than the intermetallics. As the pits propagate, due to a decrease of pH inside them the areas of attack spread causing the corrosion of the intermetallics as well and forming larger pits. The explanation for the improvement in corrosion resistance was ascribed [9] to the rapidly melting and resolidifying process related to the laser surface treatment. In the resolidifying process the solid-liquid interface moves more rapidly and entraps more solute elements than in the equilibrium solidifying process, because there is less time for the diffusion of the solute elements, thus the α-Al phase entraps more chromium, making the α-Al phase supersaturated with chromium. The presence of chromium in the passive film as CrOOH and/or Cr_2O_3 makes the film less soluble in acid solution compared to the case where only aluminium oxide exists. Thus a higher potential is needed to produce enough Al^{3+} ion that by hydrolisis increase the acidity of the solution in the pit nuclei (pre-existing film defects) and dissolve locally the film formed on the alloy containing chromium. The higher the chromium content in the laser alloyed layer, the easier the formation of a CrOOH film.

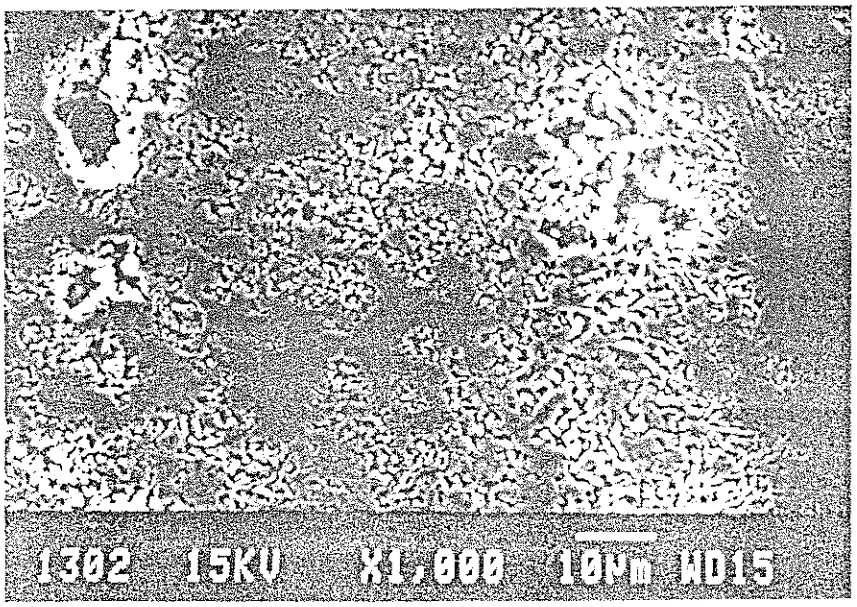

Fig. 9 - Scanning electron microgarphs showing the pitting morphologies on laser chromium-alloyed 7175 alloy [9].

Conclusions

LSM 2024

LSM of 2024 aluminium alloy produces a modified microstructure consisting of fine α-Al dendritic subgrains with Al_2Cu precipitates in the subgrain boundaries, whereas for the as received alloy the precipitates are Al_2CuMg. Since Al_2CuMg has a lower pitting potential than the α-Al grains, pitting was observed to take place at the precipitates, and this leads to intergranular corrosion. A single pitting potential was observed in the LSM alloy with pitting taking place in the α-Al dendrites rather than in the more cathodic Al_2Cu precipitates. Thus, although there is no significant increase in the critical pitting potential as a result of LSM, elimination of intergranular corrosion occurs.

LSA 7175

LSA of 7175 aluminium alloy with chromium produces a microcrystalline layer on the alloy surface with extended solubility of chromium in the α-Al phase. This element enhances the pitting corrosion resistance of the alloy by the formation of a CrOOH passive film which retards the propagation of the pitting. The higher the chromium content in the laser alloyed layer the higher the pitting potential is.

The hardness of the surface layers is remarkably enhanced by LSA with chromium.

Acknowledgement

The authors gratefully acknowledge the support received from E.C. under Contract BREU-CT 91-0494.

References

1. P.G. Moore, E. McCafferty and S.Weinman, Reports NRL Progress, 9 (Nov. 1977).
2 P.L. Bonora, M. Bassoli, P.L. De Anna, G. Battaglin, G. Della Mea, P. Mazzoldi and A. Miotello, Electrochim. Acta, **25**,1497 (1980).
3. E. McCafferty, P.G. Moore and G.T. Peace, J. Electrochem. Soc. **129**, 9 (1982).
4. S. Virtanen and H. Bohni, "Effect of Laser Surface on Passivity and its Breakdown of Al-Si Alloys", Modifications of Passive Films, (EFC12), eds.
P. Marcus, B. Baroux and M. Keddam, The Institute of Materials, London, 225 (1994).
5. P.L. Hagans and R.L. Yates, "Environmental Degradation of Ion and Laser Treated Surfaces" eds. G.S. Was and K.S. Grabowski, The Minerals Metals and Materials Soc., 215 (1989).
6. K. Urishino and K. Sugomoto, Corros. Sci., **19**, 225 (1979).
7. R. Li, A. Almeida, M.G.S. Ferreira, R. Vilar, K.G. Watkins, M.A. McMahon and W.M. Steen, "Localised Corrosion of Laser Surface Melted 2024-T351 Aluminium Alloy", Surface and Coatings Technology (in press).
8. A. Almeida, R. Vilar, R. Li, M.G.S. Ferreira, K.G. Watkins and W.M. Steen, "Laser Alloying of Aluminium and 7175 Aluminum Alloy for Enhanced Corrosion Resistance", Proceedings of the Laser Materials Processing Conference (ICALEO'93), vol. **77**, p. 903, Laser Institute of America, Orlando (1994).
9. R. Li, M.G.S. Ferreira, A. Almeida, R. Vilar, K.G. Watkins and W.M. Steen, "Localised Corrosion of Laser Surface Alloyed 7175-T7351 Aluminium Alloy with Chromium, Modification of Passive Films (EFC 12), eds. P. Marcus, B. Baroux and M. Keddam, The Institute of Materials, London, 308 (1994).